

# Universal spin-Hall conductance fluctuations in two dimensions

Wei Ren,<sup>1</sup> Zhenhua Qiao,<sup>1</sup> Jian Wang\*,<sup>1</sup> Qingfeng Sun,<sup>2</sup> and Hong Guo<sup>3</sup>

<sup>1</sup>*Department of Physics and Center of Theoretical and Computational Physics,  
The University of Hong Kong, Hong Kong, China*

<sup>2</sup>*Institute of Physics, Chinese Academy of Sciences, Beijing, China*

<sup>3</sup>*Department of Physics, McGill University, Montreal, PQ, Canada*

We report a theoretical investigation on spin-Hall conductance fluctuation of disordered four terminal devices in the presence of Rashba or/and Dresselhaus spin-orbital interactions in two dimensions. As a function of disorder, the spin-Hall conductance  $G_{sH}$  shows ballistic, diffusive and insulating transport regimes. For given spin-orbit interactions, a universal spin-Hall conductance fluctuation (USCF) is found in the diffusive regime. The value of the USCF depends on the spin-orbit coupling  $t_{so}$ , but is independent of other system parameters. It is also independent of whether Rashba or Dresselhaus or both spin-orbital interactions are present. When  $t_{so}$  is comparable to the hopping energy  $t$ , the USCF is a universal number  $\sim 0.18e/4\pi$ . The distribution of  $G_{sH}$  crosses over from a Gaussian distribution in the metallic regime to a non-Gaussian distribution in the insulating regime as the disorder strength is increased.

PACS numbers: 71.70.Ej, 72.15.Rn, 72.25.-b

The notion of dissipation-less spin-current<sup>1</sup> has attracted considerable interests recently. In its simplest form, a spin-current is about the flow of spin-up electrons in one direction, say  $+x$ , accompanied by the flow of equal number of spin-down electrons in the opposite direction,  $-x$ . The total charge current in the  $x$ -direction is therefore zero,  $I_e = e(I_\uparrow + I_\downarrow) = 0$ ; and the total spin-current is finite:  $I_s = \hbar/2(I_\uparrow - I_\downarrow) \neq 0$ . For a pure semiconductor system with spin-orbital (SO) interactions, it has been shown<sup>1</sup> that an electric field in the  $z$ -direction can induce the flow of a spin-current in the  $x$ -direction perpendicular to the electric field: such a spin-current is dissipation-less because the external electric field does no work to the electrons flowing inside the spin-current. If the semiconductor sample has a finite  $x$ -extent, the flow of spin-current should cause a spin accumulation at the edges of the sample, resulting to a situation that spin-up electrons accumulate at one edge while spin-down electrons at the opposite edge. Hence a spin-Hall effect<sup>2,3</sup> is produced where chemical potentials for the two spin channels become different at the two edges of the sample. This interesting phenomenon has been subjected to extensive studies and there are several experiments reporting spin accumulation which may have provided evidence of this effect<sup>4</sup>. It has been shown that for a pure two dimensional (2d) sample without any impurities, the Rashba SO interaction generates a spin-Hall conductivity having universal value<sup>3</sup> of  $e/8\pi$ . It has also been shown that any presence of weak disorder destroys this spin-Hall effect in the large sample limit<sup>5,6</sup>. On the other hand, numerical studies have provided evidence that for mesoscopic samples, spin-Hall conductance can survive weak disorder<sup>7,8,9</sup>.

One of the most striking quantum transport features in mesoscopic regime is the universal charge conductance fluctuation (UCF)<sup>10,11,12</sup>: quantum interference gives rise to the sample-to-sample fluctuation of charge conductance of order  $e^2/h$ , independent of the details of

the disorder, Fermi energy, and the sample size as long as transport is in the coherent diffusive regime characterized by the relation between relevant length scales,  $l < L < \xi$ . Here  $L$  is the linear sample size,  $l$  the elastic mean free path and  $\xi$  the phase coherence length. If time-reversal symmetry is broken, UCF is suppressed by a factor of two.

A very important and interesting issue therefore arises: what are the properties of the fluctuations of *spin-Hall conductance* in disordered samples? Is there a transport regime where spin-Hall conductance fluctuation is *universal*? The answers to these questions are non-trivial because the flow of dissipation-less spin-current is qualitatively different from the flow of charge current driven by an external electric field. It is the purpose of this paper to report our investigations of these issues. For a disordered four-terminal sample with a given Rashba SO interaction strength  $t_{so}$ , and/or Dresselhaus interaction strength  $t_{so2}$ , our results suggest that there is indeed a universal spin-Hall conductance fluctuation (USCF) whose root mean square amplitude is  $g = 0.18(e/4\pi)$ , independent of other system details (thus universal). The fluctuation is however a function of the SO interaction strength and found to be well fitted by a functional form of  $\text{rms}(G_{sH}) = g \tanh(|t_{so} - t_{so2}|/0.17)$ . Finally, the distribution of spin-Hall conductance obeys a Gaussian distribution in the metallic regime and deviates from it in the insulating regime.

To investigate USCF, we consider a four terminal device in two dimensions schematically shown in the left inset of Fig.1. We will first discuss the results in the presence of only Rashba interaction. In the presence of Rashba interaction ( $\alpha_{so}\mathbf{z} \cdot (\boldsymbol{\sigma} \times \mathbf{k})$ ), the Hamiltonian of

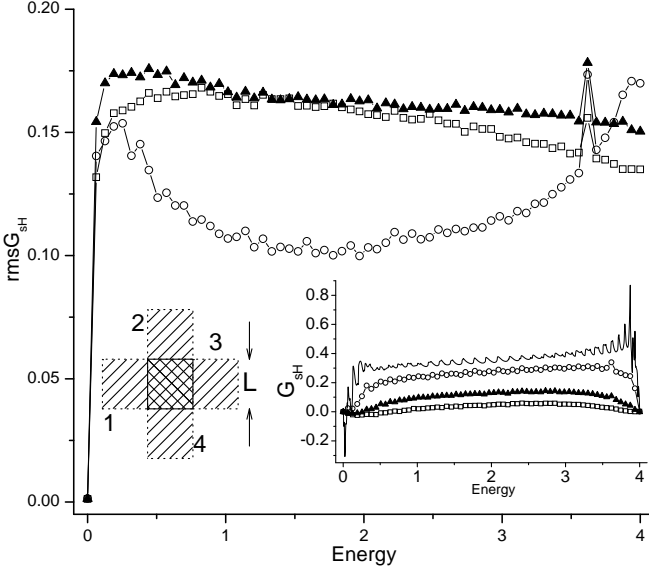


FIG. 1: Spin-Hall conductance fluctuation versus energy for disordered samples. Triangles, squares, and circles are for  $W = 1, 2, 3$  respectively. Left inset: schematic plot of the four-terminal mesoscopic sample where Rashba interaction exists in the center scattering region and the leads 1, 3. The width of the square sample is  $L$ . A small voltage bias is across leads 1,3, and spin-Hall conductance is measured through leads 2,4. Right inset: the ensemble averaged spin-Hall conductance  $G_{sH}$  versus electron energy for SO interaction strength  $t_{so} = 0.3$ . Solid line: pure sample with  $W = 0$  and other symbols are the same as the main panel. In all figures the spin conductance and its fluctuation are measured in  $e/4\pi$ .

this device is given by<sup>8</sup>:

$$\begin{aligned}
 H = & -t \sum_{\langle ij \rangle \sigma} (c_{i\sigma}^\dagger c_{j\sigma} + h.c.) + \sum_{i\sigma} \epsilon_i c_{i\sigma}^\dagger c_{i\sigma} \\
 & - t_{so} \sum_i [(c_{i,\uparrow}^\dagger c_{i+\hat{x},\downarrow} - c_{i,\downarrow}^\dagger c_{i+\hat{x},\uparrow}) \\
 & - i(c_{i,\uparrow}^\dagger c_{i+\hat{y},\downarrow} + c_{i,\downarrow}^\dagger c_{i+\hat{y},\uparrow}) + h.c.] \quad (1)
 \end{aligned}$$

where  $c_{i\sigma}^\dagger$  is the creation operator for an electron with spin  $\sigma$  on site  $i$ ,  $\hat{x}$  and  $\hat{y}$  are unit vectors along  $x$  and  $y$  directions. Here  $t = \hbar^2/2ma^2$  is the hopping energy and  $t_{so} = \alpha_{so}/2a$  is the effective spin-orbit coupling. The on-site energy is given by  $\epsilon_i = 4t$ . In addition, static Anderson-type disorder is added to  $\epsilon_i$  with a uniform distribution in the interval  $[-W/2, W/2]$  where  $W$  characterizes the strength of the disorder. We consider the situation where Rashba interaction is present everywhere except in leads 2 and 4 (see the left inset of Fig.1) in order to measure the conserved spin-current<sup>8</sup>. We apply external bias voltages at the four terminals as  $(V_i, i = 1 \cdots 4) = (v/2, 0, -v/2, 0)$ : such a setup generates a spin-current flowing from lead 2 to 4, *i.e.* a spin-Hall effect measured from these two leads<sup>8</sup>

The spin Hall conductance  $G_{sH}$  is calculated from the

Landauer-Büttiker formula<sup>7</sup>

$$G_{sH} = (e/8\pi)[(T_{2\uparrow,1} - T_{2\downarrow,1}) - (T_{2\uparrow,3} - T_{2\downarrow,3})] \quad (2)$$

where the transmission coefficient is given by  $T_{2\sigma,1} = \text{Tr}(\Gamma_{2\sigma} G^r \Gamma_1 G^a)$ , here  $G^{r,a}$  are the retarded and advanced Green's functions of central disordered region of the device which we evaluate numerically. The quantities  $\Gamma_{i\sigma}$  are the line width functions describing coupling of the leads to the scattering region, and are obtained by calculating self-energies due to the semi-infinite leads using a transfer matrices method<sup>13</sup>. The spin-Hall conductance fluctuation is defined as  $\text{rms}(G_{sH}) \equiv \sqrt{\langle G_{sH}^2 \rangle - \langle G_{sH} \rangle^2}$ , where  $\langle \cdots \rangle$  denotes averaging over an ensemble of samples with different configurations of the same disorder strength  $W$ . Note that in the presence of disorder, although one could use another the definition  $\bar{G}_{sH} = (e/4\pi)(T_{2\uparrow,1} - T_{2\downarrow,1})$  to calculate and obtain the same *average* spin-Hall conductance as that of  $G_{sH}$ , the spin-Hall fluctuation can only be obtained correctly using the definition of Eq.(2). We perform our calculations on  $L \times L$  square samples with four leads described above. Sample sizes of  $L = 40$  up to 100 are examined<sup>15</sup>. To fix units, throughout this paper we measure the energy  $E$ , disorder strength  $W$ , and spin-orbit coupling  $t_{so}$  in terms of the hopping energy  $t$ .

Fig.1 plots spin Hall conductance fluctuation vs Fermi energy at a fixed  $t_{so} = 0.3$  and sample size  $L = 40$  for several disorder strengths  $W = 1, 2, 3$ . We have also shown the averaged spin Hall conductance in the right inset. Due to the electron/hole symmetry, only data for energy range  $[0, 4]$  are shown. Over 10 000 disordered samples are averaged. For pure sample without disorder, as the Fermi energy is increased the number of subbands increase. As a result, the spin-Hall conductance  $G_{sH}$  shows small oscillations. When disorder is increased from zero,  $G_{sH}$  decreases as expected and eventually, the small oscillation due to the subbands vanishes. Most importantly, Fig.1 shows substantial sample to sample fluctuations of  $G_{sH}$ , measured by  $\text{rms}(G_{sH})$ , of the order  $\delta \frac{e}{4\pi}$  where  $\delta$  is a number between 0.1 and 0.2. Such an amplitude of fluctuation is comparable to the spin-Hall conductance itself.

In Fig.2a,b, we plot the  $\langle G_{sH} \rangle$  and  $\text{rms}(G_{sH})$  as a function of disorder strength  $W$  at fixed Fermi energy  $E = 1$  for a number of different spin-orbit couplings from  $t_{so} = 0.2$  up to 0.7. Several observations are in order. First, the spin-Hall conductance (Fig.2a) decreases smoothly as the disorder strength is increased: the transport characteristics goes from quasi-ballistic at small  $W$  to the diffusive regime at larger  $W$ . In the diffusive regime, the spin-Hall conductance decreases exponentially with the disorder strength between  $W = [1, 5]$ . Finally it goes to the insulating regime for even larger  $W$  where  $G_{sH}$  vanishes. Second, the numerical data show that the onsets of insulating regime  $W_c$  are different for different spin-orbit couplings  $t_{so}$ . The larger the spin-orbit coupling, the larger  $W_c$ . This finding is

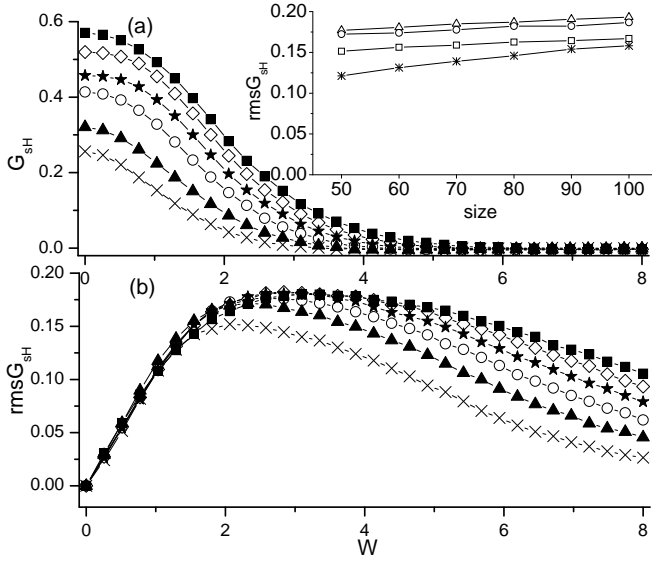


FIG. 2: (a) Ensemble averaged  $G_{sH}$  versus disorder strength  $W$  for  $t_{so} = 0.2$  (cross),  $0.3$  (filled triangle),  $0.4$  (open circle),  $0.5$  (star),  $0.6$  (rhombus),  $0.7$  (filled square). The average is over 20 000 samples with  $L = 40$ . Inset: size dependence of spin-Hall conductance fluctuation with  $t_{so} = 0.3$ . Different symbols are for  $W = 1$  (stars),  $2$  (rectangles),  $3$  (circles) and  $4$  (triangles). The ensemble average is over 20 000 samples for different size  $L$ . (b) The corresponding ensemble averaged spin-Hall conductance fluctuation versus  $W$ , the symbols are for the same  $t_{so}$  values as in (a).

consistent with that of Ref.8 which suggested that the localization length depends on  $t_{so}$  and belongs to two-parameter scaling. Third, from the spin-Hall conductance fluctuation shown in Fig.2b, we observe that for small disorder  $W < 1$ , the fluctuations for different  $t_{so}$  have very similar values and the curves collapse. For larger disorder, the fluctuations develop a plateau structure so that  $\text{rms}(G_{sH})$  becomes independent of the disorder parameter  $W$  for each given  $t_{so}$ . In this sense, the fluctuation  $\text{rms}(G_{sH})$  becomes “universal” and the spin-Hall transport enters the regime with universal spin-Hall conductance fluctuations. Importantly, both the width of the plateau and the value of USCF depend on  $t_{so}$ . The larger the  $t_{so}$ , the wider the fluctuation plateau which characterizes the diffusive regime.

Now we examine the dependence of spin-Hall conductance fluctuation  $\text{rms}(G_{sH})$  on system size  $L$  in the inset of Fig.2a for  $t_{so} = 0.3$ . With weak disorder  $W = 1$  (stars) the fluctuation increases with sample size indicating that spin-Hall conductance is not yet in the USCF regime because transport is quasi-ballistic. In the diffusive regime,  $W = 2, 3, 4$ , the fluctuations saturate at  $\delta e/4\pi$  where  $\delta \approx 0.2$ . The independence of system size by the fluctuation  $\text{rms}(G_{sH})$  provides a strong evidence of USCF. Namely, as long as transport is in the diffusive regime, the fluctuation of the spin-Hall conductance is dominated by quantum interference giving rise to a universal amplitude. Since the value of USCF

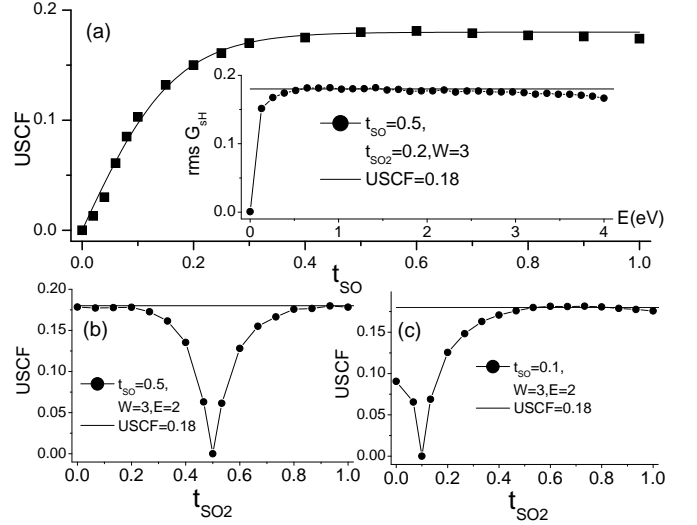


FIG. 3: (a). USCF values versus Rashba spin-orbit coupling  $t_{so}$  at  $E = 1$ . Inset:  $\text{rms} G_{sH}$  versus Fermi energy for  $W = 3$  in the presence of both Rashba and Dresselhaus SO coupling,  $t_{so} = 0.5$  and  $t_{so2} = 0.2$ . (b)/(c).  $\text{rms} G_{sH}$  versus Dresselhaus SO coupling  $t_{so2}$  at  $E = 2$ ,  $W = 3$ , and  $t_{so} = 0.5/t_{so} = 0.1$ . In the cases of inset of (a), (b) and (c), 40000 samples are collected.

(which is obtained from each curve in the lower panel of Fig.2) depends on the spin-orbit coupling  $t_{so}$  as seen from Fig.2, we have obtained a collection of the USCF for different  $t_{so}$  which is shown in Fig.3a. Interestingly, the USCF can be well fitted (solid line) by a function  $\text{rms}(G_{sH}) = g \tanh(t_{so}/0.17)$  where  $g = 0.18e/4\pi$ . This can be understood as follows. When  $t_{so} = 0$ , there is no spin-Hall current and hence no fluctuations. There is a crossover regime before the fluctuation saturates to the USCF plateau.

Fig.4a-d plot the distribution function of spin Hall conductance,  $P(G_{sH})$ , for several different disorder values  $W$ . For each  $W$ , data is accumulated by calculating 20 000 realizations of disorder.  $P(G_{sH})$  appears to clearly obey a Gaussian distribution in the metallic regime up to  $W \approx 5$ . For larger  $W$  between  $[5, 10]$ , transport is in the insulating regime, the symmetric distribution exhibits non-Gaussian behavior (Fig.4c). At even larger disorder  $W = 12$  shown in Fig.4d, the distribution becomes non-Gaussian and asymmetric. The deviation from Gaussian distribution can be characterized by the moments of spin-Hall conductance. We have calculated the skewness  $\gamma_1$  and kurtosis  $\gamma_2$  whose definitions are<sup>14</sup>,  $\gamma_1 = \mu_3/\mu_2^{3/2}$  and  $\gamma_2 = \mu_4/\mu_2^2 - 3$  where  $\mu_n = \langle (x - \langle x \rangle)^n \rangle$  ( $n = 2, 3, 4$ ) denote the central moments. The skewness describes the degree of asymmetry of a distribution around its mean while the kurtosis measures the relative peakedness of a distribution. The results are plotted in Fig.4f, showing that in the metallic regime  $W < 5$ , both skewness and kurtosis are essentially zero while they become non-zero for larger  $W$ , consistent with the distributions. Hence the skewness and kurtosis can be used to

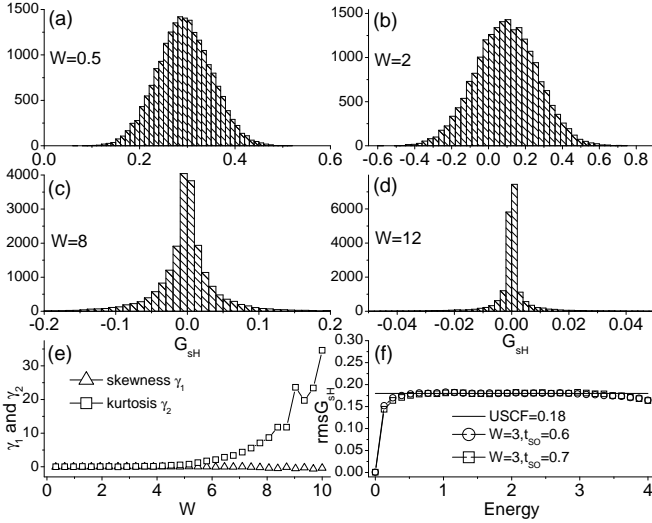


FIG. 4: (a-d) The distribution of the spin-Hall conductance for different disorder strengths at a fixed energy  $E = 1$  and  $t_{so} = 0.3$ . Data are collected for 20 000 samples for each  $W$  with  $L = 40$ . (e) The skewness  $\gamma_1$  and kurtosis  $\gamma_2$  versus disorder strength  $W$  for the same ensemble. (f)  $\text{rms} G_{sH}$  versus Fermi energy for  $W = 3$  and  $t_{so} = 0.6, 0.7$ .

identify the diffusive regime. Importantly, these quantities can be measured experimentally<sup>14</sup>. Finally, we have checked that the above features of the spin-Hall conductance fluctuation are generic and valid for other values of  $E$  and  $t_{so}$ . For instance, Fig.4f shows the  $\text{rms} G_{sH}$  versus Fermi energy when  $W = 3$  and  $t_{so} = 0.6, 0.7$ . We see that between  $E = 1$  and  $E = 3$ ,  $\text{rms} G_{sH}$  is around the universal value 0.18.

So far we have focused on spin-Hall conductance fluctuations with the Rashba interaction. To further demonstrate the universal behavior, we have also analyzed the case of Dresselhaus spin-orbital interaction by adding a term  $\beta_{so}(\sigma_x k_x - \sigma_y k_y)$  in Eq.(1). Using unitary transformations, it is easy to prove that for the spin-Hall current along z-direction we have  $I_{sH}^z(\alpha_{so} = 0, \beta_{so}) = I_{sH}^z(\alpha_{so}, \beta_{so} = 0)$  and  $I_{sH}^z(\alpha_{so} = \beta_{so}) = 0$ . When there is no Rashba spin-orbital interaction ( $\alpha_{so} = 0$ ) and only Dresselhaus term exists, we have obtained exactly the same USCF value and behavior as that of Rashba term alone. When both Rashba and Dresselhaus terms are present, it is not obvious that the USCF persists.

This is because these two terms have different symmetry, the Rashba coupling arises from the structure inversion asymmetry with SU(2) symmetry while the Dresselhaus coupling arises from the bulk inversion asymmetry with SU(1,1) symmetry<sup>16</sup>. From Fig.3b and 3c plot we see that USCF for the latter situation (both  $\alpha_{so}$  and  $\beta_{so} \neq 0$ ), the results are similar to the case of pure Rashba or pure Dresselhaus interaction. Because  $I_{sH}^z(\alpha_{so} = \beta_{so}) = 0$ , the USCF curves have a dip to zero when  $\alpha_{so} = \beta_{so}$ . Defining  $t_{so2} \equiv \beta_{so}/2a$ , Figs. 3b, 3c show that USCF is reached when  $|t_{so2} - t_{so}| \sim 0.4$ . Finally, the inset of Fig.3a shows that the USCF is independent of Fermi energy when both SO interactions are present.

In summary, for spin-Hall effect generated by the Rashba and Dresselhaus interactions in mesoscopic samples, our results strongly suggest the existence of a universal spin-Hall conductance fluctuation due to impurity scattering in the quantum coherent regime. In this regime, the USCF is characterized by sample-to-sample fluctuations of  $G_{sH}$  for a given SO interaction (Rashba or/and Dresselhaus) strength  $t_{so}$ , measured by quantity  $\text{rms}(G_{sH})$  with a *universal* amplitude  $g \equiv \delta \frac{e}{4\pi}$  where  $\delta \approx 0.18$ , which is independent of system size, impurity scattering strength, and Fermi energy. Importantly, this fluctuation amplitude is of the same order as the spin-Hall conductance itself. Comparing with the familiar UCF in charge conductance of disordered mesoscopic samples, USCF originates from a similar physics of quantum interference effect which leads to significant sample-to-sample fluctuations in spin-Hall conductance. A main difference is that spin-Hall effect is due to SO interactions in the sample, thereby the USCF also depends on the SO parameter  $t_{so}$  (or  $t_{so2}$ ), and our numerical results can be well fitted by a functional form of  $\text{rms}(G_{sH}) = g \tanh(|t_{so} - t_{so2}|/0.17)$ .

**Acknowledgments** This work was financially supported by RGC grant (HKU 7044/05P) from the government SAR of Hong Kong. Q.F.S is supported by NSF-China under Grant No. 90303016 and 10474125 and H.G is supported by NSERC of Canada, FQRNT of Québec and Canadian Institute of Advanced Research. Computer Centre of The University of Hong Kong is gratefully acknowledged for the High-Performance Computing assistance.

\*) Electronic address: jianwang@hkusub.hku.hk

<sup>1</sup> S. Murakami et al, Science **301**, 1348 (2003).

<sup>2</sup> J.E. Hirsch, Phys. Rev. Lett. **83**, 1834 (1999).

<sup>3</sup> J. Sinova et al, Phys. Rev. Lett. **92**, 126603 (2004).

<sup>4</sup> Y.K. Kato, R.C. Myers, A.C. Gossard, and D.D. Awschalom, Science **306**, 1910 (2004); J.Wunderlich, B. Kaestner, J. Sinova, and T. Jungwirth, Phys. Rev. Lett. **94**, 047204 (2005).

<sup>5</sup> J. Inoue et al, Phys. Rev. B **70**, 041303 (2004).

<sup>6</sup> E.G. Mishchenko et al, Phys. Rev. Lett. **93**, 226602 (2004).

<sup>7</sup> E.M. Hankiewicz et al, Phys. Rev. B **70**, 241301 (2004).

<sup>8</sup> L. Sheng, D.H. Sheng, and C.S. Ting, Phys. Rev. Lett. **94**, 016602 (2005).

<sup>9</sup> B.K. Nikolic et al, Phys. Rev. B **72**, 075361 (2005).

<sup>10</sup> S. Washburn and R.A. Webb, Adv. Phys. **35**, 375 (1986).

<sup>11</sup> B.L. Altshuler, Pis'ma Zh. Eksp. Teor. Fiz. **41**, 530 (1985)[JETP Lett. **41**, 648 (1985)].

<sup>12</sup> P. A. Lee and A. D. Stone, Phys. Rev. Lett. **55**, 1622 (1985).

- <sup>13</sup> M.P. López-Sancho, J.M. López-Sancho, and J. Rubio, J. Phys. F **14**, 1205 (1984); **15**, 851 (1985).
- <sup>14</sup> P. Mohanty et al., Phys. Rev. Lett. **93**, 159702 (2004).
- <sup>15</sup> Due to the extremely large computational demands for adequate ensemble averaging, very careful coding must be done to exploit the mathematical structure of the self-energy and Hamiltonian matrices which allows the Green's function to be obtained by inverting a tridiagonal matrix.

For  $L = 40$ , our code takes approximately 10 minutes to calculate a curve of spin-Hall conductance versus energy with 200 energy points on a single PC. As tests, we have reproduced results in Fig.1-3 of Ref.8.

- <sup>16</sup> J. Schliemann, J.C. Egues, and D. Loss, Phys. Rev. B **67**, 085302 (2003).